



# Tracer-free laser-induced grating spectroscopy using a pulse burst laser at 100 kHz

FRANCESCA DE DOMENICO,<sup>1</sup> THIBAUT F. GUIBERTI,<sup>2</sup> SIMONE HOCHGREB,<sup>1</sup> WILLIAM L. ROBERTS,<sup>2</sup> AND GAETANO MAGNOTTI<sup>2,\*</sup> 

<sup>1</sup>Department of Engineering, University of Cambridge, Cambridge, UK

<sup>2</sup>King Abdullah University of Science and Technology (KAUST), CCRC, Thuwal 23955-6900, Saudi Arabia

\*[gaetano.magnotti@kaust.edu.sa](mailto:gaetano.magnotti@kaust.edu.sa)

**Abstract:** This work shows the first application of a burst laser for laser-induced grating spectroscopy (LIGS) diagnostics. High repetition rate (100 kHz) LIGS is performed in non reacting and reacting flows using the fundamental harmonic of a Nd:YAG pulse-burst laser as pump. In the first part of the paper, we demonstrate the first time-resolved, high repetition rate electrostrictive LIGS measurements in a sinusoidally-modulated helium jet, allowed by the highly energetic pulses delivered by the burst laser (around 130 mJ per pulse). In the second part of the paper, we perform thermal LIGS measurements in a premixed laminar methane/air flame. Thermal gratings are generated in the flame products from the water vapour, which weakly absorbs 1064 nm light. Thus, this work demonstrates the potential of seeding-free high repetition rate LIGS as a technique to detect and time-resolve the instantaneous speed of sound, temperature, and composition in unsteady flow processes.

Published by The Optical Society under the terms of the [Creative Commons Attribution 4.0 License](https://creativecommons.org/licenses/by/4.0/). Further distribution of this work must maintain attribution to the author(s) and the published article's title, journal citation, and DOI.

## 1. Introduction

Many fundamental processes in gas dynamics, such as supersonic/hypersonic flow, combustion, aero-acoustics, and plasma physics, occur on time scales of millisecond or less, posing significant challenges for the accurate measurement of scalars such as temperature or density. To gain a deeper insight into the relevant chemical and physical quantities involved, laser diagnostics play a vital role. However, most of the pulsed lasers currently available, especially those with highly energetic pulses, operate only at low repetition rates ( $\sim 10$  Hz). The laser pulses are short and thus can measure the instantaneous behaviour, but the low repetition rate means that unsteady phenomena typical of turbulent flows cannot be captured.

Recent efforts have tried to develop high repetition rate, non-invasive techniques to measure temperature variations in reacting flows. In fact, temperature is a key parameter in combustion as it affects engine efficiency, pollutant emission, formation and destruction, and noise. However, the hostile environment of combustion chambers makes these measurements extremely challenging, so that only few experimental techniques are able to measure unsteady temperature variations without perturbing the flow. These include interferometry, laser absorption spectroscopy [1–3], Rayleigh scattering [4], Coherent Anti-Stokes Raman Spectroscopy (CARS) [5–8]. Laser-Induced Grating Spectroscopy (LIGS) offers an alternative method for gas dynamic measurements using a simpler optical arrangement, while still providing high precision and good accuracy.

LIGS is a non-linear laser diagnostic technique which measures the local speed of sound using the modulation frequency detected from probing a laser-induced transient grating. LIGS signals are based on opto-acoustic effects which arise from the interaction of the local medium with an interference pattern generated from the overlap of two pulsed laser beams. A brief description of the technique is given here; for more detail see Refs. [9–11]. LIGS signals can be generated either by a resonant or a non-resonant process. The non-resonant process arises

from an electrostrictive interaction named Laser-Induced Electrostrictive Grating Scattering (LIEGS) whereas the resonant process arises from resonant absorption of the radiation energy, and subsequent collisional quenching, leading to Laser-Induced Thermal Grating Scattering (LITGS). When the excitation is rapid, two counter-propagating acoustic waves are generated leading to a periodic modulation of the grating scattering efficiency. The frequency of these oscillations depends on the local speed of sound and is detected by the first-order Bragg scattering of a probe beam. The energies required to generate the thermal gratings are normally one order of magnitude lower than those needed to generate the electrostrictive gratings. Although LITGS typically offers a higher signal to noise ratio than LIEGS, its main limitation is the need for sufficient concentration of a resonant species at the available pump laser wavelength. Much of the previous literature has covered LIGS measurements using low repetition rate, high power lasers. Only recent experiments have demonstrated LITGS at frequencies up to 10 kHz [12,13] using high repetition rate PIV lasers. As these pump lasers could only deliver low-energy pulses (1-5 mJ), a strong absorber at the laser wavelength had to be seeded into the flow in order to generate thermal LIGS signals. Such energies were too weak to generate detectable electrostrictive gratings, so there have been no high repetition rate electrostrictive LIGS measurements yet.

In this work, for the first time, a pulse burst Nd:YAG laser [14] is used as pump to generate LIGS signals. A burst laser generates high repetition rate (10-100 kHz) pulses for a short amount of time (a burst of pulses over a time of 10 ms), followed by a cooling time between bursts of 10-20 s. Using the fundamental harmonic of the Nd:YAG laser (1064 nm), the energy of each pulse, of the order of 100 mJ, is sufficient to generate detectable electrostrictive gratings. High repetition rate-time resolved electrostrictive LIGS measurements are obtained for the first time in a sinusoidally modulated helium-air jet, highlighting advantages and disadvantages of such application. Then, as a proof of concept, 100 kHz LIGS is applied to a premixed methane/air flame in a vessel at 4 bar. In this case, a thermal grating is generated by the absorption of light at 1064 nm by weak water vapor lines, aided by the presence of percent levels of water in the reaction product mixture. The 100 kHz data is compared with measurements previously performed at 10 Hz [15], to verify accuracy and precision, and demonstrate that 100 kHz LIGS diagnostics using pulse burst lasers can be successfully applied in flames.

## 2. Experimental set-up

### 2.1. Optical arrangement

The optical layout of the experiment is sketched in Fig. 1 and is briefly described here (for a more detailed description refer to [15]). The  $\lambda = 1064$  nm pump laser pulses were generated at 100 kHz with a Nd:YAG pulse-burst laser (Quasimodo<sup>TM</sup> from Spectral Energies). A 10 Hz Nd:YAG laser (Continuum Powerlite DLS9010) was used for comparison. A movable mirror on a magnetic base allowed switching between the two laser sources while using the same optical arrangement. Further on, a 50/50 beam splitter plate optimized for 1064 nm divided the beam into two identical beams. These two parallel beams, separated by 50 mm, were crossed using a 75-mm diameter bi-convex crossing lens (CL) with a 750-mm focal length, resulting in a crossing angle  $\theta \approx 3.81^\circ$ . This arrangement produced a grating of  $\Lambda = (\lambda/2)/\sin(\theta/2) = 16 \mu\text{m}$  spacing in a probe volume of length and width of approximately 4 mm and 200  $\mu\text{m}$ , respectively. The expected LIGS frequency  $f$  is calculated as:

$$f = \frac{nc}{\Lambda} = \frac{n}{\Lambda} \sqrt{\frac{\gamma RT}{W}} \quad (1)$$

where  $c$  is the local speed of sound,  $n = 1$  for thermal gratings and  $n = 2$  for electrostrictive gratings,  $\gamma$  is the specific heat capacity ratio,  $R$  the universal gas constant,  $T$  the local temperature, and  $W$  the molar mass. The probe beam was generated by a continuous wave solid state laser

(Coherent Verdi G) operating at 532 nm with a power output of 2 W and a diameter of  $\sim 2$  mm. A guide beam, also at 532 nm, produced by a diode laser (Thorlabs CPS532) was used as a tracer to identify the direction of the scattered signal and facilitate positioning of the collection optics. These four beams (two pumps, the probe, and the tracer beams) were coplanar and alignment masks were used to adjust their respective positions. The LIGS signal was collected by a PMT (Hamamatsu H10721-20). Two 550 nm low pass filters (T: 99.9% at 532 nm, T: 0.08% at 1064 nm) were mounted in front of the PMT to improve the rejection of background scattered light. An infrared photodiode (Thorlabs DET210) detected the pump pulses and triggered acquisition of the LIGS signal. The PMT and photodiode signals were recorded using an oscilloscope (Keysight DSOS804A, 10 Gs/s sampling rate, 8 GHz bandwidth).

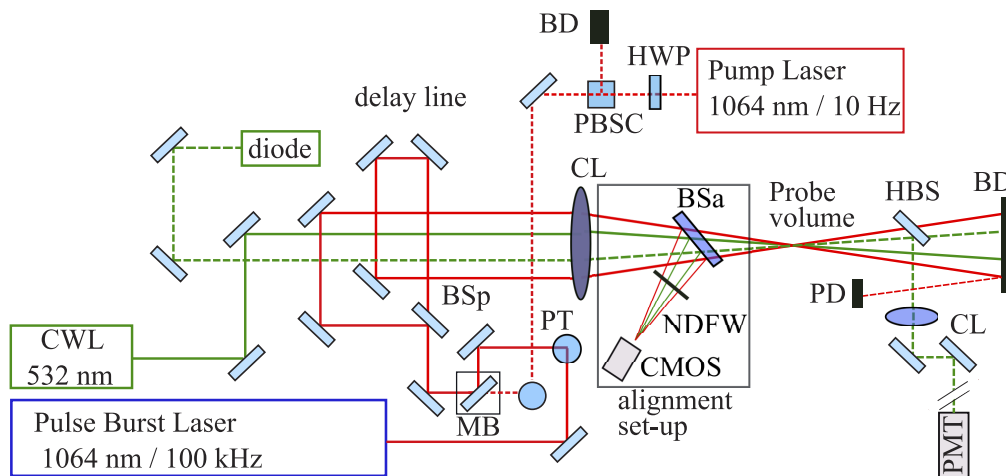


**Fig. 1.** Optical layout of the experiment. BSp: Beam Splitter (for 1064 nm); PT: Periscope Tower; MB: Magnetic Base; CL: Crossing Lens; BD: Beam Dump; PBSC: Polarising Beam Splitter; HWP: Half Wave Plate; BSa: Beam Sampler; NDFW: Neutral Density Filter Wheel; CMOS: CMOS Camera; HBS: Harmonic Beam Splitter; PMT: Photomultiplier. Refer to [15] for more details.

## 2.2. Experimental rigs

LIEGS measurements were performed over a modulated jet of helium and air (Fig. 2(a)). A flow of helium (5 SLPM) was continuously delivered into a plenum, which was then connected to a 3/8" vertical pipe. A loudspeaker driven at 300 Hz modulated the helium flow entering the pipe. At a distance of 200 mm downstream of the exit of the plenum, a steady flow of air from a choked valve (10 SLPM) was added to the helium flow using a T-junction. The air-helium mixture then travelled through the metal pipe for 200 mm before exiting into the room. The probe volume was located in the center of the jet, 3 mm above the exit of the pipe. In addition to electrostrictive LIGS measurements in a non-reactive jet, thermal LIGS measurements were performed at 100 kHz and 10 Hz in laminar premixed methane/air flat flames produced with a McKenna burner. The burner was located in a vertically-oriented pressure vessel operated at 4 bar (Fig. 2(b)). A detailed description of the vessel with the burner can be found in [15].

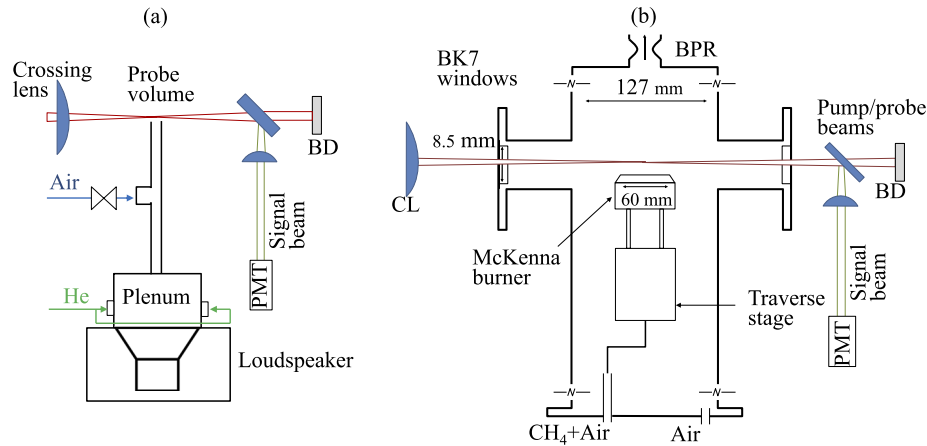


**Fig. 2.** Experimental set-up: Helium jet (a) and pressure vessel with McKenna burner (b).  
CL: Crossing Lens; BPR: Back Pressure Regulator; BD: Beam Dump

### 3. Experimental results

#### 3.1. High repetition rate LIEGS measurements in a helium/air jet

Time-resolved, high repetition rate LIEGS measurements were performed in the helium/air jet, where the concentration of helium was periodically modulated at 300 Hz with the loudspeaker, changing, in turn, both the specific heat capacity ratio and the molar mass of the mixture, and therefore the local speed of sound in the flow passing through the probe volume. The pulse burst laser was operated at a repetition rate of 100 kHz, delivering 1000 pulses of 130 mJ each (10 ms burst duration). The cooling time between bursts was set to 20 s.

As helium and air molecules do not absorb 1064 nm radiation, no thermal gratings were formed in the probe volume, but electrostrictive signals were generated as the energies delivered by the pulses of the burst laser were sufficiently high. Figure 3(a) shows two single shot normalized LIEGS signals obtained in jets with different compositions: the red signal was acquired in pure air (which was used for calibration), while the black signal was acquired in the steady mixture of air and helium, with a helium concentration of 6.3% by mass. The different densities of the two jets (and consequently the different speeds of sound) were reflected in the different oscillation frequencies and the different damping rates of the two signals. In the mixture with helium, both the speed of sound and the damping rate of the signals were higher, due to the lower density of the gas in the probe volume [11].

Measurements were taken in the steady jet of air, air and helium and in the modulated jet of air and helium. The loudspeaker was driven with a sinusoidal wave input but, due to the rather large input amplitude used, the modulated flow did not display a perfect sinusoidal shape. Figure 3(b) shows the time-resolved (non averaged) normalized density  $\rho/\rho_0$  derived from the LIEGS signals during a burst using the following procedure. Let  $f_{E,0}$  be the calibration frequency, which is acquired in pure air. For each LIEGS shot in the mixture, the instantaneous molar concentration of helium in the probe volume  $X_{He}$  is determined from its frequency  $f_{E,i}$  using Eq. (1) [13]:

$$\left(\frac{f_{E,i}}{f_{E,0}}\right)^2 = \frac{\left(1 - \frac{R}{\bar{c}_{p,a}(1-X_{He}) + \bar{c}_{p,h}X_{He}}\right)^{-1}}{\left(1 - \frac{R}{\bar{c}_{p,a}}\right)^{-1}} \frac{W_a}{W_a(1 - X_{He}) + W_{He}X_{He}} \quad (2)$$

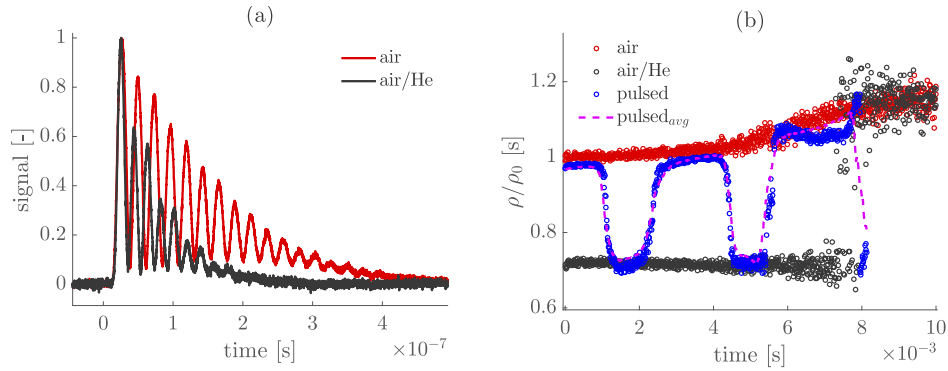


**Fig. 3.** Normalized single shot LIGS signals recorded at 100 kHz in the steady jets of air (red) and helium and air (black) (a). Density derived from LIGS signals during a 10 ms burst (b): steady jet of pure air (red circles), steady mixture of helium and air (black circles); modulated jet of helium and air (blue circles) and corresponding averaged signal over 42 bursts (magenta line).

Assuming constant temperature, the knowledge of  $X_{He}$  allows the determination of the instantaneous density  $\rho_i$ , as follows:

$$\frac{\rho_i}{\rho_0} = \frac{W_i}{W_a} = \frac{W_a(1 - X_{He}) + W_{He}X_{He}}{W_a} \quad (3)$$

where  $\bar{c}_p$  is the specific molar heat capacity at constant pressure,  $(\ )_a$  refers to pure air,  $(\ )_{He}$  to pure helium. In Fig. 3, the red dots correspond to the air-only jet; the black circles to the jet of air and helium (6.3 % in mass) and the blue circles to the sinusoidally modulated jet (time-resolved measurements), while the magenta line shows an average in the oscillating jet over 42 bursts.

### 3.1.1. Drift in the probe volume

A drift in the inferred density can be observed by looking at the evolution of the density derived from the LIGS signals over the burst (Fig. 3(b)). The behaviour of the signals during the burst suggests that such a drift was not caused by a physical change in the local conditions owing to e.g. laser-induced thermalisation. For the signal in air (red dots) the derived density shows an apparent positive increase during the burst, which would correspond to a local temperature decrease that can not attributed to any external changes caused by the laser. The apparent change in density was instead caused by a drift in the spatial location and crossing angle of the beams forming the probe volume. In fact, images of the laser beam during the burst reveal that the beam is affected by a spatial drift, becoming also somewhat defocused. This effect is attributed to the high radiation energy and the consequent thermal loading that a burst generates on the amplifiers and optics (both inside and outside the laser). As the two beams travel for about 2 m before crossing in the probe volume, even small initial shifts can be highly amplified along the path, and this can substantially affect the crossing angle and consequently the grating spacing, as well as the spatial location of the probe volume.

Images of the beam revealed that its drift is consistent from burst to burst, so that, in principle, the effect of change in the crossing angle can be removed from the data by using a calibration in steady air. As the speed of sound in steady air  $c_a$  can be assumed to be constant, the variation of the LIGS frequency  $f_{a,i}$  at each shot  $(\ )_i$  should only reflect the variation of the crossing angle  $\theta_i$  and consequently of the grating spacing  $\Lambda_i$ :

$$f_{a,i} = \frac{c_a}{\Lambda_i} = c_a \frac{\sin(\theta_i/2)}{\lambda/2} \quad (4)$$

This quantity  $\Lambda_i$  can be used to obtain the *correct* speed of sound  $c_{E,i}$  in each shot during the burst as:

$$c_{E,i} = \Lambda_i f_{E,i} \quad (5)$$

From Eq. (4), the crossing angle had changed by 5% between the beginning and the end of the burst. The data is also more scattered at the end of the burst: the overlap between the three beams (two pump and probe beams) had deteriorated, making the quality of the signal poorer. In particular, the biggest variation occurs after  $t = 5$  ms, thus, this effect might be mitigated by reducing the duration of the burst.

After applying the correction of Eq. (5), only the variation of the crossing angle has been considered, but not the spatial change in the position of the probe volume. The beam drift had moved the probe volume away from the centre of the jet, therefore the data at the beginning and at the end of the burst were not acquired at the same location. In this experiment, this movement is particularly evident in the last milliseconds of the burst in the helium-air jet (black dots in Fig. 3(b)): the probe volume had travelled out of the jet completely until it reached the still air, as evidenced by the acquired density which corresponds to air. Additionally, for the sinusoidally-modulated flow, in the first two periods of oscillations generated by the speaker, the acquired density variation has a clearer shape, while in the last one it is distorted. Variations in the length and location of the probe volume might also change the overall composition of the mixture inside it (higher or lower percentage of helium). This could explain why the opposite behaviour in the derived density is observed in the jet of pure air and helium and air: the concentration of helium in the probe volume may vary between the beginning and the end of the burst. This reduces the spatial resolution that can be achieved with the measurements and hinders the acquisition of local phenomena occurring at a specific point. Care must be taken while choosing the experimental target, which has to be large enough to ensure that the probe volume remains inside it during a burst and has uniform properties in the measurement plane (or at least in the area where the probe volume is expected to move).

This simple experiment shows how the data acquired with a burst laser should be carefully evaluated to ensure that variations due to the misalignment of the system are not erroneously confused with physical changes in the properties the flow. As final remark, it has to be clarified that this is not an inherent limitation of the technique, but of the current state of the art of the lasers. Improvements in the instrumentation, such as a better stability of the burst laser, and more robust optical components might help to reduce this issue.

### 3.2. High repetition rate LIGS measurements in flames

Here we compare the speed of sound and water concentration derived from LIGS signals using the 100 kHz pulse burst laser and the 10 Hz laser (the results obtained with the 10 Hz laser are discussed in [15]). The measurements were performed in a steady laminar flame due to a limitation of the pressure vessel, which could not sustain the flow rates required for turbulent/unsteady flames. Water available in the flame products weakly absorbs 1064 nm light, generating a detectable thermal grating at such energies, and a weaker, but non-negligible, electrostrictive grating.

LIGS was used to determine the local speed of sound and water concentration in the products of lean-to-rich premixed methane-air flames at 4 bar. The measurements shown here were conducted 5 mm above the surface of the burner, in the product zone. A total of 200 pulses of 130 mJ each were delivered at 100 kHz from the pulse burst laser. This burst duration was chosen to reduce the thermal load on the windows of the vessel and also to make the effect of the beam drift less severe. Figure 4(a) shows ensemble averaged LIGS signals for the same flame (with an equivalence ratio of  $\phi = 0.95$ ) obtained with the high (black) and low (red) repetition rate lasers. The thermal (T) and electrostrictive (E) peaks are marked on the figure. The two signals display a nominally identical oscillation frequency. The small differences in the frequencies are

due to the differences in the crossing angles of the pump beams in the low and high speed set-up. These variations are taken into account during the corresponding calibrations in still air. The two signals show the same number of peaks, but they differ in their contrast (e.g. peak-to-valley amplitude ratio), due to the differences in the pulse width of the two lasers [11].

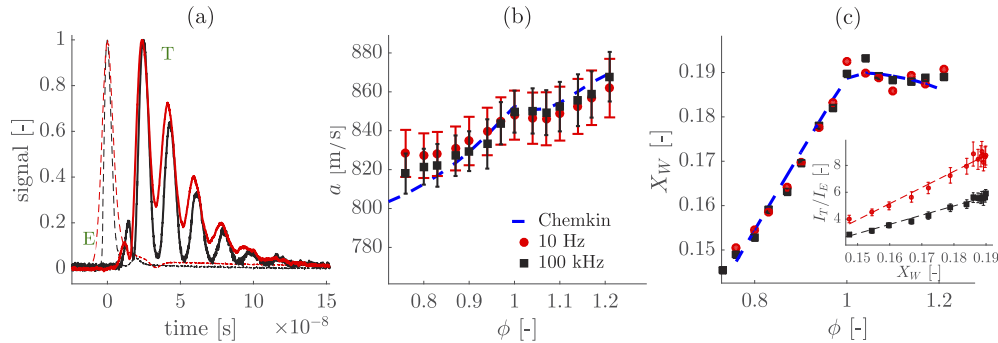


**Fig. 4.** Comparison between 100 kHz (black) and 10 Hz (red) LIGS measurements in premixed methane-air flames at 4 bar. Normalized LIGS signals (solid line) and pump laser pulses (dashed lines) (a); measured speed of sound (b); measured water concentration (c).

The equivalence ratio in the flames was varied from  $\phi = 0.73$  to  $\phi = 1.30$  by varying the fuel mass flow rate while keeping the air mass flow rate constant to verify accuracy and precision. Figure 4 compares the speed of sound (b) and water concentration (c) obtained from LIGS signals with the 100 kHz and the 10 Hz laser and with predictions from burner-stabilized flame simulations using Chemkin. The speed of sound is extracted from the oscillation frequency of the signals, according to Eq. (1). The water concentration is derived after calibration using the intensity ratio of the thermal to electrostrictive peaks in the signal, as explained in [15]. The inset in Fig. 4(c) shows the calibration curves for determining the water concentration. The calibration curves obtained for the two laser sources are both linear but they have a different slope due to the different signal contrasts. Results at high and low repetition rate agree by 0.2-1.2% for the speed of sound and by 0.2-1.7% for the water concentration, and also show good agreement with the Chemkin calculations discussed in [15], suggesting that high repetition rate measurements of temperature and water concentration can be made in reacting flows using a 1064 nm pulse burst laser and water as an absorber.

#### 4. Conclusions

For the first time, tracer-free LIGS measurements are demonstrated at rates of 100 kHz using a pulse burst laser. The energies delivered at the fundamental harmonic (around 130 mJ per pulse) allow the generation of detectable electrostrictive gratings. Here we present the first time-resolved LIGS measurements in a sinusoidally-modulated, non reacting helium-air jet. This simple experiment highlights an issue regarding the stability of the laser: the high energies used to pump the laser amplifier cause a drift in the direction of the laser beam, which manifests itself as a drift in the acquired frequency of LIGS signals, limiting the useful burst duration. In the second part of the paper, to demonstrate the potential of the technique in reacting flows, a comparison between high and low repetition rate LIGS measurements was made in premixed methane-air flames at 4 bar. The water vapour naturally produced by the flame weakly absorbs the 1064 nm laser light, generating a thermal grating. The speed of sound and water concentration measurements at 100 kHz compare well with results at 10 Hz, demonstrating that LIGS can be potentially used as a tool to detect and time-resolve unsteady changes in turbulent reacting flows. In conclusion, this work demonstrates a significant improvement in the time resolution

obtainable using LIGS. To the authors' knowledge, energies higher than 100 mJ per pulse (which are typically required to generate electrostrictive signals using folded boxcars arrangements) at 10-100 kHz can be delivered only by burst lasers, which allow repetition rates at least one order of magnitude higher than conventional high-speed PIV lasers.

## Funding

King Abdullah University of Science and Technology; Engineering and Physical Sciences Research Council (EP/K02924X); KAUST visiting students program; University of Cambridge.

## Acknowledgments

The help of Dr. Yedhu Krishna with the pulse burst laser and Anthony Bennet with the pressure vessel was highly appreciated.

## Disclosures

The authors declare no conflicts of interest.

## References

1. M. G. Allen, "Diode laser absorption sensors for gas-dynamic and combustion flows," *Meas. Sci. Technol.* **9**(4), 545–562 (1998).
2. D. F. Davidson, A. Y. Chang, M. D. Dirosa, and R. K. Hanson, "Continuous wave laser absorption techniques for gas-dynamic measurements in supersonic flows," *Appl. Opt.* **30**(18), 2598–2608 (1991).
3. R. K. Hanson and D. F. Davidson, "Recent advances in laser absorption and shock tube methods for studies of combustion chemistry," *Prog. Energy Combust. Sci.* **44**, 103–114 (2014).
4. G. H. Wang, N. T. Clemens, and P. L. Varghese, "High-repetition rate measurements of temperature and thermal dissipation in a non-premixed turbulent jet flame," *Proc. Combust. Inst.* **30**(1), 691–699 (2005).
5. S. Roy, W. D. Kulatilaka, D. R. Richardson, R. P. Lucht, and J. R. Gord, "Gas-phase single shot thermometry at 1-kHz using fd-CARS spectroscopy," *Opt. Lett.* **34**(24), 3857–3859 (2009).
6. S. Roy, J. R. Gord, and A. K. Patnaik, "Recent advances in coherent anti-Stokes Raman scattering spectroscopy: Fundamental developments and applications in reacting flows," *Prog. Energy Combust. Sci.* **36**(2), 280–306 (2010).
7. S. Roy, P. Hsu, N. Jiang, M. N. Slipchenko, and J. R. Gord, "100-kHz-rate gas-phase thermometry using 100-ps pulses from a burst-mode laser," *Opt. Lett.* **40**(21), 5125–5128 (2015).
8. J. D. Miller, M. S. Slipchenko, J. G. Mance, and R. S. J. Gord, "1-kHz two-dimensional coherent anti-Stokes Raman scattering (2D-CARS) for gas-phase thermometry," *Opt. Express* **24**(22), 24971–1342 (2016).
9. E. B. Cummings, I. A. Leyva, and H. G. Hornung, "Laser-induced thermal acoustics (LITA) signals from finite beams," *Appl. Opt.* **34**(18), 3290–3302 (1995).
10. H. Latzel, A. Dreizler, T. Dreier, J. Heinze, M. Dillmann, W. Stricker, G. M. Lloyd, and P. Ewart, "Thermal grating and broadband degenerate four-wave mixing spectroscopy of OH in high-pressure flames," *Appl. Phys. B: Lasers Opt.* **67**(5), 667–673 (1998).
11. A. Stampanoni-Panariello, D. N. Kozlov, P. P. Radi, and B. Hemmerling, "Gas phase diagnostics by laser-induced gratings I. Theory," *Appl. Phys. B: Lasers Opt.* **81**(1), 101–111 (2005).
12. F. J. Förster, C. Crua, M. Davy, and P. Ewart, "Time-resolved gas thermometry by laser-induced grating spectroscopy with a high-repetition rate laser system," *Exp. Fluids* **58**(7), 87 (2017).
13. F. De Domenico, S. M. Lowe, L. Fan, B. A. O. Williams, and S. Hochgreb, "High frequency measurement of temperature and composition spots with LITGS," *J. Eng. Gas Turbines Power* **141**(3), 1–11 (2019).
14. P. P. Wu and R. B. Miles, "High-energy pulse-burst laser system for megahertz-rate flow visualization," *Opt. Lett.* **25**(22), 1639–1641 (2000).
15. F. De Domenico, T. F. Guiberti, S. Hochgreb, and W. L. Roberts, "Temperature and water measurements in flames using 1064 nm Laser-Induced Grating Spectroscopy (LIGS)," *Combust. Flame* **205**, 336–344 (2019).